Formation of the New Trigonal Polymorph in iPP−1-Hexene Copolymers. Competition with the Mesomorphic Phase

María L. Cerrada, María J. Polo-Corpa, Rosario Benavente, and Ernesto Pérez*

Instituto de Ciencia y Tecnología de Polímeros (CSIC), Juan de la Cierva 3, 28006-Madrid, Spain

Teresa Velilla and Raúl Quijada

Departamento de Ingeniería Química, Facultad de Ciencias Físicas y Matemáticas, Universidad de Chile, Casilla 2777, and Centro para la Investigación Multidisciplinaria Avanzada en Ciencias de los Materiales (CIMAT), Santiago, Chile

Received September 24, 2008; Revised Manuscript Received November 20, 2008

ABSTRACT: The polymorphic structure and the thermal transitions of several iPP−1-hexene copolymers have been analyzed by performing DSC and variable-temperature X-ray diffraction experiments. Special attention has been paid to the range of "intermediate" comonomer contents, between around 8 and 12 mol %, where the new trigonal form of iPP starts to be observed. It was found that the mesomorphic modification is also easily obtained in that comonomer range, so that the possibility of such mesomorphic phase acting as a transient structure of the trigonal form was entertained. However, the results have clearly shown that the mesomorphic modification is not acting as such transient structure, and rather it is a competitor (as well as the α crystals) for the formation of the trigonal phase.

Introduction

Isotactic polypropylene, iPP, exhibits an amazing polymorphism, depending on microstructural features, crystallization conditions, and other factors like the use of specific nucleants. Thus, three different polymorphic modifications, α, β, and γ, all sharing a 3-fold conformation,[1−4] have been reported. In addition, fast quenching of iPP leads to a phase of intermediate or mesomorphic order.[1,4−9]

It is well established that the monoclinic α form[10] is the most common and stable modification, being found in all kinds of solution-crystallized iPP samples and also in most melt-crystallized specimens.[1,2,4,10,11] The trigonal β modification[12,13] is a metastable phase that does not appear on the phase diagram,[14,15] and it is produced only under special crystallization conditions or in the presence of selective β nucleating agents.[1−4,16−18] The orthorhombic γ form[19] has been found in the case of low-molecular-weight iPP and in random copolymers of propylene and α-olefins[1,2,4,11,20] or by the effect of pressure.[14,15,21,22] Moreover, the γ modification is especially favored in the case of iPP synthesized by metallocene catalysts because of the presence of errors homogeneously distributed among the different polymer chains.[23−26]

As usual in polymer crystallization, both thermodynamic and kinetic considerations are of capital importance for the obtainment of a certain modification, and it is usual to observe a competition between the different polymorphs.[27]

In addition to those four modifications, a new trigonal form has been recently reported[28−34] in the case of copolymers of iPP with high contents of 1-hexene or 1-pentene as comonomers. The use of metallocene catalysts makes possible the synthesis of such copolymers with a homogeneous distribution of comonomer.[28,34] In those reports, and focusing the attention in iPP−1-hexene copolymers, the new trigonal modification is the only one obtained for comonomer contents above around 14 mol %, while variable proportions of it with the α modification were found in the comonomer range from around 8 to 13 mol % 1-hexene.

The reason given for the obtainment of this new trigonal polymorph is the substantial inclusion of comonomer units in the crystals, which is only produced when the comonomer content is high enough. But, is this the only reason?

In recent years there has been also an increasing interest in considering the polymer crystallization as a multistage process via an intermediate mesomorphic phase.[35−37] Foundations for this scheme are based on the Ostwald's rule of stages, formulated more than 100 years ago.[38] This empirical rule states that a phase transformation will proceed through metastable states, whenever they exist, and it has been recently invoked in the crystallization of different materials[39] and specifically for polymer crystallization[35,36] by combining both phase stability and kinetic considerations. These arguments have been applied to the crystallization of a liquid crystalline copolyester[40] finding rather interesting differences between the crystals obtained from the isotropic melt or from an intermediate smectic mesophase.

Since a kind of mesomorphic structure is also involved in the crystallization of iPP, and considering that the quenching conditions for its obtainment are getting more and more mild as the comonomer content increases, as will be shown below, our original hypothesis was that such mesomorphic phase may exert a certain influence on the formation of the new trigonal polymorph.

The aim of this paper is, therefore, the analysis of that possible influence, by studying the polymorphic structure and thermal transitions of iPP−1-hexene copolymers. Special attention will be paid to the range of intermediate comonomer contents, between around 8 and 12 mol %.

Experimental Part

Copolymerizations of propylene with 1-hexene were performed as described elsewhere[41,42] with toluene as a solvent in a Slurry system in 1 L Buchi glass reactor, using the *rac*-$Me_2Si(2\text{-}Me\text{-}Ind)_2ZrCl_2$/MAO catalytic system. The results, determined by ^{13}C NMR spectroscopy, about either comonomer or stereodefect contents found in the different samples analyzed are shown in Table 1. The different copolymers were labeled as CPH followed by a number that specifies their comonomer molar fractions.

* Corresponding author. E-mail: ernestop@ictp.csic.es.

10.1021/ma802170a CCC: $40.75
Published on Web 01/20/2009

Table 1. Characterization of the Different Samples

sample	comonomer content (mol %)	% mmmm	% mmmr	M_w (kg/mol)
iPP	0	95.0	2.2	224
CPH0.9	0.9	94.7	1.8	215
CPH2.9	2.9	95.0	1.2	174
CPH8.6	8.6	96.1	1.0	183
CPH11.3	11.3			136

The molecular weights were determined by gel permeation chromatography in a Waters 150 CV-plus system equipped with an optical differential refractometer (model 150 C). A set of three columns of the Styragel HT type (HT3, HT4, and HT6) was used with 1,2,4-trichlorobenzene as a solvent. Standards of polystyrene and polyethylene with narrow molecular mass distribution were used for calibration. The results are also shown in Table 1.

Films were obtained by compression molding in a Collin press between hot plates (at a temperature of around 40 °C above the melting point) at a pressure of 1 MPa for 4 min. Two different thermal treatments were applied. The first thermal history consisted of a slow cooling from the molten state down to room temperature, at the inherent cooling rate of the press, after the power was switched off. The second one was a relatively fast cooling between plates refrigerated with cold water after the melting of the material in the press.

The thermal properties of the different specimens were analyzed in a Perkin-Elmer DSC-7 calorimeter connected to a cooling system and calibrated with different standards. The sample weight ranged from 6 to 9 mg, and different heating and cooling rates were used.

Wide-angle X-ray diffraction (WAXD) patterns were recorded in the reflection mode by using a Bruker D8 Advance diffractometer provided with a Goebel mirror and a PSD Vantec detector (from Bruker, Madison, WI). Cu Kα radiation was used. The equipment was calibrated with different standards. A first series of diffractograms were registered at room temperature, on the different samples prepared as films under the two thermal treatments described above. Those samples had been at room temperature at least for 4 months. A step scanning mode was employed for the detector, with a 2θ step of 0.024° and 0.2 s per step.

Variable-temperature experiments were also performed on selected specimens. In this case, an Anton-Paar TTK-450 chamber, provided with a liquid nitrogen regulator and a vacuum pump, was employed as temperature controller, and three different acquisition modes were used: (a) A step-temperature mode: the temperature was raised in steps of 10 °C (at a rate of 10 °C/min), and after 5 min for temperature equilibration the diffractograms were acquired under the step scanning mode for the detector (time between diffractograms around 10 min). (b) A real-time mode: the temperature was raised at a fixed, continuous nominal rate of 10 °C/min, while, simultaneously, the diffractograms were collected with the PSD in the fixed scan position, covering the 2θ range from around 9.3 to 19°, and with a total time between diffractograms of 15 s, so that real-time variable-temperature experiments are collected, with a temperature resolution between frames of around 2 °C. (c) A mixed mode, where the temperature is changed gradually (at a nominal rate of 2 °C/min on cooling and 10 °C/min on heating) while the detector was in the step scanning mode, but now at the maximum scanning rate allowed by the software: 0.05 s per step, so that the total acquisition time of a diffractogram is around 1 min.

Results and Discussion

The X-ray diffractograms of the different samples slowly cooled from the melt are shown in Figure 1. As expected, and considering the metallocenic nature of the catalyst employed in the synthesis, the homopolymer exhibits the diffractions characteristic of both the α and γ modifications of iPP. Other features in this figure are also in accord with published work. First, the γ content increases for low comonomer contents, but decreases, and eventually disappears at higher contents.[33]

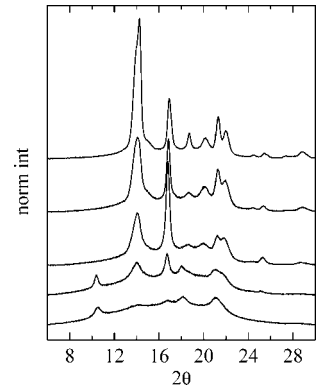

Figure 1. X-ray diffractograms, at room temperature, for the different samples slowly cooled from the melt. From top to bottom: iPP, CPH0.9, CPH2.9, CPH8.6, and CPH11.3, respectively.

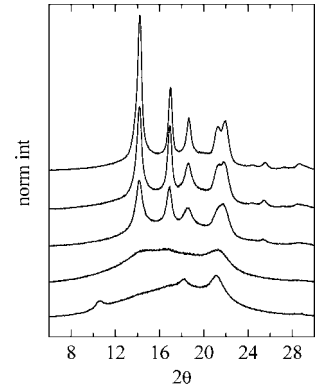

Figure 2. X-ray diffractograms, at room temperature, for the different samples rapidly cooled from the melt. From top to bottom: iPP, CPH0.9, CPH2.9, CPH8.6, and CPH11.3, respectively.

Second, the crystallinity decreases with the increase of comonomer content. And, finally, both the α modification and the new trigonal form (with its most differentiating diffraction at 2θ around 10.5°) are observed for the two copolymers with high comonomer content: CPH8.6 and CPH11.3.

On the other hand, Figure 2 shows the diffractograms corresponding to the samples rapidly cooled from the melt. As usual,[23,24,27] the γ phase is hardly observed in these samples with fast cooling. However, some unexpected features are deduced from this figure. A plausible hypothesis is that the new trigonal form has to compete with the α modification, so that the crystallization conditions leading to a depletion of the α content should lead to higher amounts of trigonal form. However, the results in Figure 2 indicate that this hypothesis is not correct. Thus, the diffractogram for copolymer CPH8.6 is characteristic of the mesomorphic modification[1] of iPP (with a minor amount of α crystals). Although this sample has been at room temperature for more than 1 year after its preparation, no sign of the diffraction at around 10.5° (trigonal form) is observed.

On the contrary, the previous hypothesis seems to be fulfilled by copolymer CPH11.3, since the diffractogram of the specimen of this copolymer rapidly cooled from the melt indicates a majority of trigonal form and only a very minor amount of α modification, if any (see lower diffractogram in Figure 2).

Trying to understand the reasons behind these "contradictory" behaviors, several variable-temperature X-ray diffraction experiments were planned, focusing the attention on copolymers CPH8.6 and CPH11.3.

Prior to this study, the different samples were analyzed by DSC. Figure 3a shows the DSC melting curves corresponding

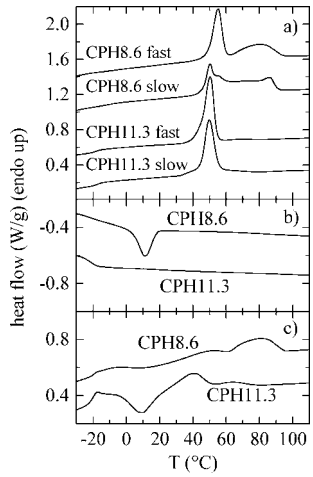

Figure 3. DSC curves corresponding to the indicated specimens: (a) first melting curves of the two processing conditions (fast and slow cooling) of copolymers CPH8.6 and CPH11.3; (b) curves on cooling from the melt and (c) subsequent heating. Cooling and heating rate: 10 °C/min.

to both the slowly and rapidly cooled specimens of copolymers CPH8.6 and CPH11.3. The four curves are not very different, with a more prominent endothermic peak centered at around 50 °C. This peak has been traditionally assigned to the melting of those crystals reorganized during the long time annealing at room temperature. We will come back to the real origin of this peak later on.

On the other hand, Figure 3b shows the DSC curves for those two copolymers on cooling from the melt at 10 °C/min, and the subsequent heating, again at 10 °C/min, is shown in Figure 3c. Regarding the cooling curves, it can be observed that CPH8.6 exhibits a relatively intense exotherm centered at around 11 °C, with its low-temperature tail very close, or overlapping, to the glass transition. On the contrary, no exotherm is observed for copolymer CPH11.3, and only the glass transition appears in its cooling curve; i.e., this copolymer does not crystallize appreciably on cooling at 10 °C/min. However, its subsequent heating curve exhibits a cold crystallization peak, centered at around 10 °C, followed by two small endotherms at 40 and 63 °C.

The heating curve for copolymer CPH8.6 shows also a small cold crystallization peak, indicating that the crystallization process was not completed on cooling, and again two endotherms are observed, now at 50 and 80 °C.

An additional experiment was performed on copolymer CPH11.3, by cooling from the melt at a smaller rate: 2 °C/min. The corresponding DSC cooling curve and its subsequent melting (again at 10 °C/min) are shown in Figure 4. Now, a crystallization exotherm is observed at around 0 °C, but clearly overlapping with the glass transition, in such a way that also a cold crystallization peak appears on heating.

With all this information, variable-temperature X-ray diffraction experiments were performed on those two copolymers of interest. For practical reasons, different kinds of experiments were carried out: step-temperature and real-time ones. The first kind had the advantage of acquiring the entire diffractogram, with a proper signal-to-noise ratio, working with the PSD detector as a goniometer. The second ones are superior in what they are real-time and simulate perfectly the DSC experiments, working with the PSD in fixed position, but the covered 2θ window is only of around 10°.

Figures 5 and 6 present the diffractograms in the step-temperature mode corresponding to the specimens of copolymer CPH8.6 slowly and rapidly cooled, respectively. Although only

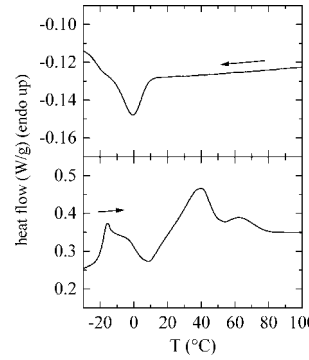

Figure 4. DSC curves on cooling at 2 °C/min (upper frame) and on the subsequent heating at 10 °C/min (lower frame) of sample CPH11.3.

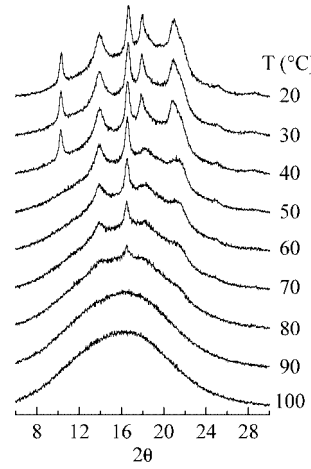

Figure 5. X-ray diffractograms, at the indicated temperatures, corresponding to the heating, in a step-temperature mode, of specimen CPH8.6 slowly cooled from the melt.

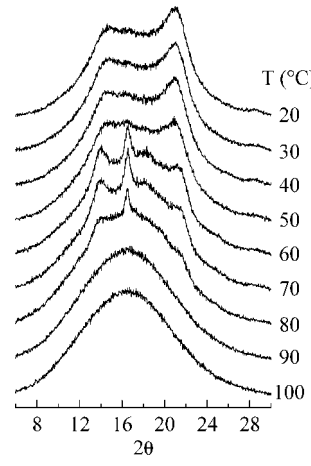

Figure 6. X-ray diffractograms, at the indicated temperatures, corresponding to the heating, in a step-temperature mode, of specimen CPH8.6 rapidly cooled from the melt.

semiquantitative conclusions can be extracted from these experiments, a rather clear picture of the very big differences among these two specimens of the same copolymer is evident. Thus, Figure 5 indicates that the trigonal modification melts at around 50 °C, and the remaining α crystals survive up to around 90 °C. On the contrary, the diffractograms in Figure 6 for the rapidly cooled specimen show that the mesomorphic phase recrystallizes into the α form again at around 50 °C, and the α crystals melt at 90 °C. Previous works on conventional iPP

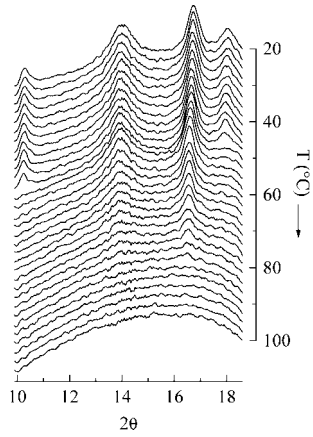

Figure 7. X-ray diffractograms corresponding to the heating at 10 °C/min, in a real-time mode, of specimen CPH8.6 slowly cooled from the melt.

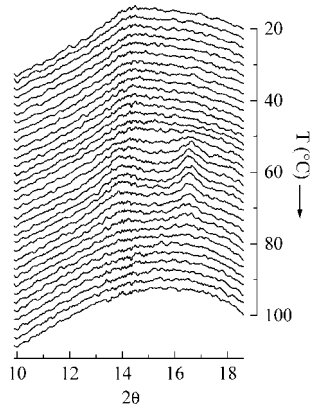

Figure 8. X-ray diffractograms corresponding to the heating at 10 °C/min, in a real-time mode, of specimen CPH8.6 rapidly cooled from the melt.

homopolymer reported[9,43,44] that the mesomorphic to α transition appears as an exothermic peak centered at around 100 °C, and the final melting of the α crystals occurs at around 162 °C.

More precise temperature information is deduced from the real-time experiments shown in Figures 7 and 8, where the two specimens of copolymer CPH8.6 are heated at a rate of 10 °C/min, acquiring diffractograms every 15 s. The thermal transitions of the different modifications can be easily obtained individually from these experiments, by monitoring the intensity of selected diffraction peaks: the ones at around 10.3°, 14.3°, and 16.7° were chosen for the trigonal, mesomorphic, and α modifications, respectively.

The results deduced from the melting experiment in Figure 7, i.e., for specimen CPH8.6 slowly cooled from the melt, are shown in Figure 9. Since trigonal and α crystals are present in this sample, the intensity and position of the diffractions at $2\theta = 10.3°$ and 16.7° have been determined as a function of temperature. The upper frame in Figure 9 represents the variation of the position of the two peaks. As expected, a small decrease of the angle (a small increase of the corresponding Bragg spacing) is observed when the temperature increases, as corresponds to a thermal expansion.

More interesting is the evolution of the area of those two peaks (Figure 9b). It can be observed that the trigonal peak vanishes at around 52 °C, while the α diffraction intensity begins to decrease also at around 50 °C, melting completely at 90 °C. It follows, therefore, that the trigonal crystals melt directly, and

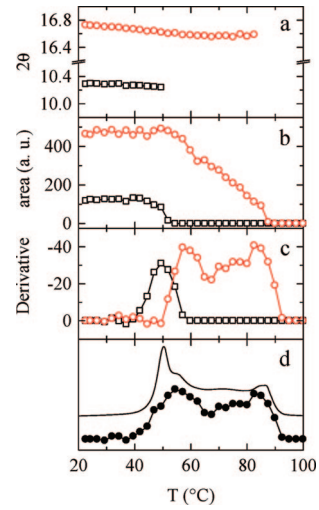

Figure 9. Temperature dependence of different parameters from the heating experiment of Figure 7 corresponding to specimen CPH8.6 slowly cooled from the melt: (a, b, and c) position, area, and derivative of the area, respectively, of the two selected diffractions for the α (circles) and trigonal forms (squares); (d) comparison of the normalized derivative (see text) of the areas of the two selected diffraction peaks (solid circles) with the DSC melting curve (continuous line).

they do not recrystallize into the α form. On the other hand, the derivative of the areas of those two peaks is displayed in Figure 9c. These derivative curves are more intuitive for the analysis of the transition temperatures, since they resemble somehow the DSC curves.

There is another aspect, however, that must be considered when trying to extract more quantitative information. The areas in Figure 9b refer to those of the selected diffraction peaks, and it can be observed that the initial area of the selected α peak is around 3 times bigger than the one for the trigonal peak. If we come back to Figure 5, where the entire diffractograms are displayed, and considering that the profile of the molten sample is also registered, the fractional X-ray crystallinity of both the α and the trigonal modifications can be estimated. Thus, the diffractogram at 20 °C involves a 71% of amorphous profile, while that at 50 °C, where the trigonal crystals have disappeared, is composed of 86% of amorphous component. The conclusion is, therefore, that sample CPH8.6 slowly cooled from the melt is composed of around 15% of trigonal crystals, 14% of α crystals, and 71% of amorphous component.

If the areas in Figure 9b are scaled with these numbers, and the derivatives are then made, and the values for the two modifications are added, the final result is displayed in Figure 9d, compared to the corresponding DSC melting curve (with the *Y* scale arbitrarily chosen). The resemblance between the two curves is noticeable, although the resolution in the DSC curve is better. Nevertheless, the results from the X-ray diffractograms are more interesting since we can extract unambiguous information about the melting of the two modifications separately.

On the other hand, the results deduced from the diffractograms in Figure 8 for specimen CPH8.6 rapidly cooled from the melt are shown in Figure 10. The monitoring of the mesomorphic peak at 14.3° is not very informative, since it overlaps with an α diffraction. Anyway, the top frame in Figure 10 represents the position of the maximum around 14°−14.3° as a function of temperature. The discontinuity observed at 55 °C indicates clearly the transformation of the mesomorphic phase into the α form.

More interesting for the analysis of the phase transitions is the variation of the α peak at around 16.7°. This peak is practically undetectable until the temperature reaches around

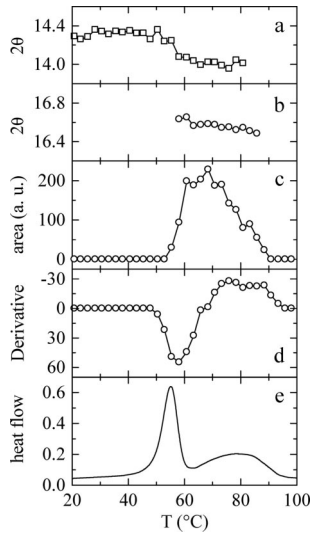

Figure 10. Temperature dependence of different parameters from the heating experiment of Figure 8 corresponding to specimen CPH8.6 rapidly cooled from the melt: (a) position of the diffraction at around 14° (corresponding initially to the mesomorphic phase and later to the α modification); (b, c, and d) position, area, and derivative of the area, respectively, of the diffraction at around 16.7° (corresponding to the α modification); (e) DSC melting curve.

55 °C, when the mesomorphic phase recrystallizes into the α modification, and it survives up to 90 °C, when it melts completely.

The variation of the position and intensity of this diffraction is displayed in parts b and c of Figure 10, respectively. The corresponding derivative of the area is shown in Figure 10d compared to the DSC melting curve (Figure 10e). Again, the real-time X-ray results are superior, since the recrystallization of the mesomorphic phase into α crystals is not inferred from the DSC melting curve, because it does not go below the baseline (exothermic). However, the derivative of the X-ray results clearly shows that recrystallization, prior to the final melting of the α crystals.

Regarding copolymer CPH11.3, the real-time X-ray experiments on the two specimens (slowly and rapidly cooled from the melt) do not show any additional interesting feature. The slowly cooled sample exhibits both trigonal and α crystals (lower diffractogram in Figure 1), the trigonal ones melting at around 50 °C and the α crystals disappearing completely at around 80 °C. As to the rapidly cooled sample (lower diffractogram in Figure 2), the majority of the crystals are now of the trigonal type, which melt again at around 50 °C, and a very minor amount of α crystals is left, melting at around 70 °C, in agreement with the DSC results in Figure 3.

However, the subsequent crystallization from the melt turned out to be more interesting than expectations. Thus, from the DSC cooling curves in Figures 3 and 4 (and from the cooling curves, not shown, for the other copolymers with lower 1-hexene content), it seems to be deduced that, on cooling from the melt at a typical DSC rate of 10 °C/min, the exotherm corresponding to the nonisothermal formation of the α crystals occurs at a temperature that decreases with increasing comonomer content. This is trivial. Moreover, when the comonomer content is higher than around 11 mol %, no crystallization exotherm is observed at that cooling rate, and this rate has to be reduced to observe crystallization on cooling, as happens in Figure 4 for copolymer CPH11.3 cooled at 2 °C/min. The logical assumption is that α crystals are again formed.

However, the DSC experiments in Figure 4 were reproduced in the X-ray diffractometer. Since now the cooling rate is only 2 °C/min, variable-temperature experiments were programmed,

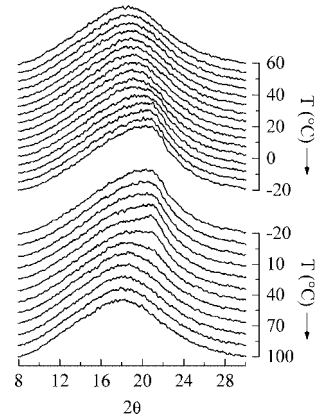

Figure 11. X-ray diffractograms, in a mixed mode (see Experimental Part), corresponding to sample CPH11.3 on cooling from the melt at 2 °C/min (upper) and subsequent heating at 10 °C/min (lower).

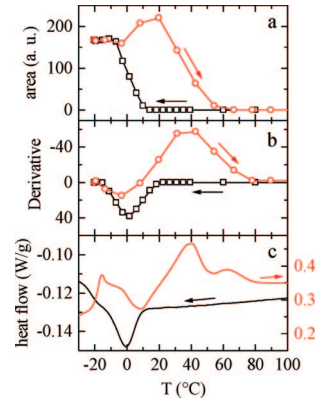

Figure 12. Temperature dependence of different parameters from the cooling (squares) and heating (circles) experiments of Figure 11 corresponding to sample CPH11.3: (a) area of the diffraction at around 21°; (b) derivative of that area; (c) corresponding DSC curves.

with continuous cooling, but with the detector acting as a goniometer, acquiring the entire diffractograms. Thus, the temperature resolution on cooling is good enough, although the one on heating, at 10 °C/min, is much poorer.

The corresponding diffractograms are shown in Figure 11. Surprisingly, what crystallizes at around 0 °C is the mesomorphic phase and not the α crystals. Even more, the lower part of Figure 11 shows the diffractograms in the subsequent melting. Surprisingly again the cold crystallization on melting observed in the DSC curve (see Figure 3) corresponds once more to the formation of additional amounts of mesomorphic phase (characterized by a relatively broad diffraction at around 21°), and this phase melts directly, with no sign of α phase formation on heating.

The evolution of that mesomorphic diffraction with temperature is shown in Figure 12. The upper frame represents the variation of its area during the cooling and subsequent melting, and the derivative of that area is displayed in Figure 12b. The resemblance with the DSC curves (Figure 12c) is evident, especially for the cooling experiment, since the melting part of the X-ray results involves a rather low temperature resolution.

The important findings are therefore (a) when cooling at relatively low rates, sample CPH11.3 leads to the mesomorphic phase and not to α crystals, and (b) the mesomorphic phase melts directly, and its transformation into the α phase on heating is not observed.

Another interesting aspect, coming back to the DSC melting curves in Figure 3, is the origin of the main melting peaks at

around 50 °C. It was commented above that it is usually attributed to the melting of those crystals (α crystals) reorganized by annealing at room temperature. This is certainly true for copolymers of low comonomer content. However, the results obtained here for copolymers CPH8.6 and CPH11.3 indicate that the dominant contribution of this peak may have well different origins: either is due to the melting of trigonal crystals or to the disappearance of the mesophase.

A final aspect refers to the influence of the mesomorphic phase on the formation of the trigonal form. It is well known[1,4] that the mesomorphic phase in iPP homopolymer is obtained under very fast quenching conditions. However, as the comonomer content increases, the quenching conditions are getting milder, as shown above. Thus, Figure 2 indicates that copolymer CPH8.6 leads almost to the pure mesomorphic modification by cooling in the press with refrigerating water, while the homopolymer and the other copolymers with smaller comonomer content lead to the α polymorph. Moreover, Figure 11 shows that the mesomorphic phase is obtained for copolymer CPH11.3 when cooling from the melt at 2 °C/min (and no α phase is identified), although that formation takes place below room temperature.

Since the minimum 1-hexene content where the trigonal polymorph is observed coincides with the region where the mesomorphic phase is easily obtained, one of the aims of this work was to analyze a possible relation between the formations of these two phases. Even more, one of our original hypotheses was that the mesomorphic phase could act as a transient phase for the trigonal modification. The results presented here, however, indicate that the mesomorphic phase is not acting as a transient structure, and rather it is a competitor of the trigonal modification.

A more detailed analysis of the mesomorphic phase characteristics of these copolymers, and of other iPP copolymers with different comonomer, is under study, considering the relatively high importance of this phase at intermediate or high comonomer contents.

Some interesting conclusions can be extracted from all the previous information. First, the α crystals are not the only competitors of the trigonal form for these iPP−1-hexene copolymers of "medium" comonomer content: the influence of the mesomorphic phase is also very important.

Second, it is presumed that in a narrow comonomer content interval around 11 mol % the mesomorphic formation is faster than that of the α crystals at "normal" cooling rates. A crossover of the actual free energy curves of these two modifications seems to occur at this comonomer content, in such a way that, on heating, the mesomorphic phase does not transform into α crystals, as it happens for iPP homopolymer and for the copolymers with lower comonomer contents (CPH8.6 for instance).

Third, fortunately the formation of the mesomorphic phase in such case occurs below room temperature. This turns out to be of capital importance for the development of the trigonal modification, since a normal crystallization procedure involves the cooling from the melt to room temperature at a certain rate and the subsequent crystallization (a slow process[30]) at ambient conditions in order to obtain the trigonal modification. Under such circumstances, the mesomorphic phase will not be a competitor for the formation of the trigonal crystals.

Fourth, at higher comonomer contents (above around 13 mol % considering the published data[28,30]) the cooling from the melt at normal experimental rates will lead to amorphous samples, and neither the α crystals nor the mesophase is formed. The trigonal modification is, therefore, free to be developed, without competitors.

Incidentally, the other possible competitor is the γ modification. However, the results in Figure 2 indicate that this modification is not observed in the rapidly cooled samples, as commented above. Moreover, and in agreement with other literature reports, the diffractograms in Figure 1 for the slowly cooled samples show that the amount of γ form increases first for low comonomer contents,[25,33] but it disappears[33] when the comonomer content is higher than around 9 mol %. Therefore, at high contents the γ modification is not a competitor.

Acknowledgment. The financial support of MEC (Projects MAT2005-00228 and MAT2007 65519-C02-01) and of CONICYT (project FONDAP 11980002) is gratefully acknowledged. We also thank the assistance of Dr. G. Galland in the ^{13}C NMR experiments.

References and Notes

(1) Brückner, S.; Meille, S. V.; Petraccone, V.; Pirozzi, B. *Prog. Polym. Sci.* **1991**, *16*, 361.
(2) Lotz, B.; Wittmann, J. C.; Lovinger, A. J. *Polymer* **1996**, *37*, 4979.
(3) Varga, J. *J. Mater. Sci.* **1992**, *27*, 2557.
(4) Phillips, P. J.; Mezghani, K. In *The Polymeric Materials Encyclopedia*; Salamone, J. C., Ed.; CRC Press: Boca Raton, FL, 1996; Vol. *9*, p 6637.
(5) Slichter, W. P.; Mandell, E. R. *J. Appl. Phys.* **1958**, *29*, 1438.
(6) Hosemann, R.; Wilke, W. *Makromol. Chem.* **1968**, *118*, 230.
(7) Grebowicz, J.; Lau, J. F.; Wunderlich, B. *J. Polym. Sci., Polym. Symp.* **1984**, *71*, 19.
(8) Corradini, P.; de Rosa, C.; Guerra, G.; Petraccone, V. *Polym. Commun.* **1989**, *30*, 281.
(9) Arranz-Andrés, J.; Benavente, R.; Pérez, E.; Cerrada, M. L. *Polym. J.* **2003**, *35*, 766.
(10) Natta, G.; Corradini, P. *Nuovo Cimento Suppl.* **1960**, *15*, 40.
(11) Turner-Jones, A.; Aizlewood, J. M.; Beckett, D. R. *Makromol. Chem.* **1964**, *75*, 134.
(12) Meille, S. V.; Ferro, D.; Brückner, S.; Lovinger, A. J.; Padden, F. J. *Macromolecules* **1994**, *27*, 2615.
(13) Lotz, B.; Kopp, S.; Dorset, D. C. R. *Acad. Sci. Paris, Ser. IIb* **1994**, *319*, 187.
(14) Mezghani, K.; Phillips, P. J. *Polymer* **1998**, *39*, 3735.
(15) Dimeska, A.; Phillips, P. J. *Polymer* **2006**, *47*, 5445.
(16) Keith, H. D.; Padden, F. J.; Walter, N. M.; Wyckoff, H. W. *J. Appl. Phys.* **1959**, *30*, 1485.
(17) Varga, J. In *Polypropylene: Structure, Blends and Composites*; Karger-Kocsis, J., Ed.; Chapman and Hall: London, 1995; Vol. *1*, p 56.
(18) (a) Varga, J. *J. Macromol. Sci., Phys. B* **2002**, *41*, 1121. (b) Varga, J.; EhrensteinW. In *Polypropylene: An A-Z Reference*; Karger-Kocsis, J., Ed.; Kluwer: London, 1999; p 51.
(19) Brückner, S.; Meille, S. V. *Nature (London)* **1989**, *340*, 455.
(20) Addink, E. J.; Beintema, J. *Polymer* **1961**, *2*, 185.
(21) Bruckner, S.; Phillips, P. J.; Mezghani, K.; Meille, S. V. *Macromol. Rapid Commun.* **1997**, *18*, 1.
(22) Mezghani, K.; Phillips, P. J. *Polymer* **1997**, *38*, 5725.
(23) Pérez, E.; Zucchi, D.; Sacchi, M. C.; Forlini, F.; Bello, A. *Polymer* **1999**, *40*, 675.
(24) Alamo, R. G.; Kim, M.-H.; Galante, M. J.; Isasi, J. R.; Mandelkern, L. *Macromolecules* **1999**, *32*, 4050.
(25) Hosier, I. L.; Alamo, R. G.; Esteso, P.; Isasi, J. R.; Mandelkern, L. *Macromolecules* **2003**, *36*, 5623.
(26) De Rosa, C.; Aurienma, F.; Paolillo, M.; Resconi, L.; Camurati, I. *Macromolecules* **2005**, *38*, 9143.
(27) Krache, R.; Benavente, R.; López-Majada, J. M.; Pereña, J. M.; Cerrada, M. L.; Pérez, E. *Macromolecules* **2007**, *40*, 6871.
(28) Poon, B.; Rogunova, M.; Hiltner, A.; Baer, E.; Chum, S. P.; Galeski, A.; Piorkowska, E. *Macromolecules* **2005**, *38*, 1232.
(29) Lotz, B.; Ruan, J.; Thierry, A.; Alfonso, G. C.; Hiltner, A.; Baer, E.; Piorkowska, E.; Galeski, A. *Macromolecules* **2006**, *39*, 5777.
(30) De Rosa, C.; Dello Iacono, S.; Auriemma, F.; Ciaccia, E.; Resconi, L. *Macromolecules* **2006**, *39*, 6098.
(31) De Rosa, C.; Auriemma, F.; Corradini, P.; Tarallo, O.; Dello Iacono, S.; Ciaccia, E.; Resconi, L. *J. Am. Chem. Soc.* **2006**, *128*, 80.
(32) De Rosa, C.; Auriemma, F.; Ruiz de Ballesteros, O.; Resconi, L.; Camurati, I. *Chem. Mater.* **2007**, *19*, 5122.
(33) De Rosa, C.; Auriemma, F.; Ruiz de Ballesteros, O.; De Luca, D.; Resconi, L. *Macromolecules* **2008**, *41*, 2172.
(34) De Rosa, C.; Auriemma, F.; Talarico, G.; Ruiz de Ballesteros, O. *Macromolecules* **2007**, *40*, 8531.
(35) Keller, A.; Hikosaka, M.; Rastogi, S.; Toda, A.; Barham, P. J.; Goldbeck-Wood, G. *J. Mater. Sci.* **1994**, *29*, 2579.

(36) (a) Strobl, G. *Prog. Polym. Sci.* **2006**, *31*, 398. (b) Strobl, G. *Eur. Phys. J.* **2000**, *3*, 165.
(37) Stribeck, N.; Bayer, R.; Bösecke, P.; Almendarez-Camarillo, A. *Polymer* **2005**, *46*, 2579.
(38) Ostwald, W. *Z. Phys. Chem.* **1897**, *22*, 286.
(39) Stoica, C.; Verwer, P.; Meekes, H.; Vlieg, E.; van Hoof, P. J. C. M.; Kaspersen, F. M. *Int. J. Pharm.* **2006**, *309*, 16.
(40) Fernández-Blázquez, J. P.; Pérez-Manzano, J.; Bello, A.; Pérez, E. *Macromolecules* **2007**, *40*, 1776.
(41) Quijada, R.; Guevara, J. L.; Galland, G. B.; Rabagliati, F. M.; López-Majada, J. M. *Polymer* **2005**, *46*, 1547.
(42) López-Majada, J. M.; Palza, H.; Guevara, J. L.; Quijada, R.; Martínez, M. C.; Benavente, R.; Pereña, J. M.; Pérez, E.; Cerrada, M. L. *J. Polym. Sci., Part B: Polym. Phys.* **2006**, *44*, 1253.
(43) Vittoria, V. *J. Macromol. Sci., Phys.* **1989**, *B28*, 489.
(44) O'Kane, W. J.; Young, R. J.; Ryan, A. J.; Bras, W.; Derbyshire, G. E.; Mant, G. R. *Polymer* **1994**, *35*, 1352.

MA802170A